Cardenas Morales, BK, Forrest, J, Castro Aponte, WV, Sanchez Cornejo, HE, La Torre, B, Jhoncon Kooyip, J, Byrne, P, Nguyen, TT, Barnes, CHW and De Los Santos Valladares, L

Geochemical, hydrochemical and remote sensing study of an Andean calcareous wetland in Huanta, Peru

Article

Journal of Hydrology: Regional Studies 62 (2025) 102767

Contents lists available at ScienceDirect

Journal of Hydrology: Regional Studies

journal homepage: www.elsevier.com/locate/ejrh

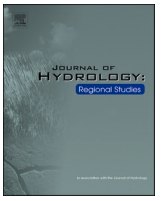

Geochemical, hydrochemical and remote sensing study of an Andean calcareous wetland in Huanta, Peru

Bruno K. Cardenas Morales [a,*], John Forrest [b], Walter V. Castro Aponte [a], Henry E. Sanchez Cornejo [c], Braulio La Torre [d], Jorge Jhoncon Kooyip [e], Patrick Byrne [f], T.T. Nguyen [g], Crispin H.W. Barnes [b], Luis De Los Santos Valladares [b,*]

[a] Escuela Profesional de Ingeniería y Gestión Ambiental, Universidad Nacional Autónoma de Huanta, Jr. Manco Cápac 497, Huanta, Ayacucho, Peru
[b] Cavendish Laboratory, Department of Physics, University of Cambridge, 19 J.J. Thomson Ave., Cambridge CB3 0US, UK
[c] Laboratorio de Cerámicos y Nanomateriales, Facultad de Ciencias Físicas, Universidad Nacional Mayor de San Marcos, Ap. Postal 14-0149, Lima, Peru
[d] Facultad de Agronomía, Universidad Nacional Agraria de la Molina, Lima, Peru
[e] Centro de Investigación en Agricultura Orgánica, Universidad Nacional de Educación Enrique Guzmán y Valle, Chosica, Lima 15472, Peru
[f] School of Biological and Environmental Sciences, Liverpool John Moores University, Liverpool L3 3AF, UK
[g] College of Natural Sciences, Can Tho University, 3-2 Road, Can Tho City 94000, Vietnam

ARTICLE INFO

Keywords:
Calcareous wetland
Hydrochemical variability
Sediment geochemistry
Remote sensing
Redox stability
Early degradation

ABSTRACT

Study region: The Huaper Wetland is located in the Huanta Province, Ayacucho Region, in the Central Peruvian Andes at 2353 m above sea level. This calcareous highland ecosystem has a key role for irrigation, biodiversity conservation, and local water supply. However, it is increasingly affected by unregulated tourism, agricultural runoff, and poor waste management.

Study focus: This study presents the first integrated geochemical, hydrochemical, and remote sensing assessment of the Huaper Wetland. Water samples were collected during four campaigns across two hydrological years (March and November 2023–2024), representing both Austral summer and winter. Parameters analyzed included pH (6.92–7.22), electrical conductivity (0.87–0.94 dS/m), total dissolved solids, dissolved oxygen (min. 1.43 mg/L), and potentially toxic elements. Seventeen sediment samples were characterized using Energy Dispersive X-ray Spectroscopy (EDX) and X-ray Diffraction (XRD), confirming dominance of calcite (up to 43.8 %) and magnesium calcite (32.8 %), with traces of nitratine ($NaNO_3$) suggesting agricultural influence. Surface moisture dynamics were assessed using the Normalized Difference Water Index (NDWI) from Sentinel-2 imagery (2016–2023).

New hydrological insights for the region: The results indicate initial signs of water quality deterioration, with nitrate levels in November 2023 (8.09 mg/L) exceeding national standards and a decline in the Water Quality Index from "Excellent" (94.92–100.00) in 2023 to "Good" (92.04) in 2024. NDWI analysis revealed a persistent decrease in surface moisture, with a minimum in 2017 (–0.4699; STD = 0.0716). Elevated sodium concentrations and low dissolved oxygen levels may destabilize redox conditions, potentially mobilizing arsenic and lead. These findings suggest a weakening of the wetland's geochemical buffering capacity and highlight the urgency of

* Corresponding authors.
E-mail addresses: 2112810108@unah.edu.pe (B.K. Cardenas Morales), ld301@cam.ac.uk (L. De Los Santos Valladares).

https://doi.org/10.1016/j.ejrh.2025.102767
Received 30 June 2025; Received in revised form 7 September 2025; Accepted 8 September 2025
Available online 16 September 2025

implementing land-use regulation, salinity control, and cost-effective long-term monitoring in calcareous Andean wetlands.

1. Introduction

Wetlands are essential yet increasingly vulnerable ecosystems that perform critical ecological functions such as regulating hydrological cycles, supporting biodiversity, and contributing to climate change mitigation (Dangles et al., 2017). Acting as natural reservoirs, biogeochemical filters, and refuges for endemic species, wetlands sustain both ecological integrity and socio-economic balance. However, these systems are under growing pressure from human activities such as agricultural expansion, informal tourism, and inefficient waste management, which lead to hydrological and geochemical alterations (Dinsa and Gemeda, 2019; Kingsford, 2016; Khatri, 2013).

Among wetland types, calcareous wetlands are particularly notable for their carbonate-rich composition, especially the presence of calcite ($CaCO_3$). These wetlands exhibit high alkalinity, strong pH buffering, and a natural ability to retain potentially toxic elements such as arsenic and lead through adsorption and co-precipitation (House and Denison, 2002; Flower et al., 2021; Wang, 2020). These characteristics make them ecologically valuable, particularly in regions affected by agriculture or mining. Despite their importance, calcareous wetlands at high altitudes in the tropical Andes remain understudied—especially in terms of their mineralogical stability and their responses to land-use and climate variability.

The Huaper Wetland was selected for this study due to its classification as a high-altitude calcareous system (2353 m a.s.l.)—a rare wetland type in the Central Andes with exceptional geochemical buffering capacity. In addition to its carbonate-rich sediments, it exhibits a shallow water table, lacks permanent inflows or outflows, and undergoes seasonal recharge mainly from orographic precipitation. These hydrogeomorphic features, combined with its small surface area (~8.4 ha) and ecological sensitivity, make Huaper an ideal sentinel site for detecting early signals of wetland degradation.

In the high Andes, previous research has focused primarily on floristic inventories and basic hydrochemical assessments (Erwin, 2009; Xi et al., 2021). However, recent studies from Argentina, Bolivia, and Chile—including those in regions impacted by lithium mining—have revealed progressive salinization, ionic imbalances, and declining ecosystem resilience (Wetlands, 2024). These regional trends underscore the importance of integrated monitoring approaches capable of capturing subtle, early-stage geochemical changes before irreversible thresholds are crossed.

The Huaper Wetland, located in the province of Huanta in the central Peruvian Andes at 2353 m above sea level, provides ecosystem services such as groundwater recharge, irrigation support, and habitat provision (Cardenas Morales et al., 2025). Despite these functions, the site lacks formal environmental oversight. It is not included in national monitoring frameworks like the *Registro Nacional de Ecosistemas Frágiles* or the *Programa de Monitoreo de Humedales* (MINAM, 2022), and agencies such as the National Water Authority (ANA) do not conduct systematic evaluations. This lack of institutional attention reflects a broader management gap affecting small or non-designated wetlands across the Andes.

Field evidence suggests that Huaper faces increasing pressures from diffuse agricultural runoff, unregulated tourism, and poorly managed solid waste. These stressors appear linked to measurable declines in water quality—including salinity increases, oxygen depletion, and shifts in sediment geochemistry (Dubuc et al., 2017). However, it remains unclear whether these changes stem from surface inputs, groundwater upwelling, or a combination of both. Moreover, no baseline dataset currently exists to inform long-term evaluation or policy interventions.

Although Huaper is not formally protected under national wetland inventories, its characteristics align with the conservation priorities defined in Peru's *National Wetlands Strategy* (D.S. 004–2015-MINAM), which emphasizes protection of carbonate-rich high-altitude wetlands exposed to seasonal recharge and land-use stress. This broader relevance strengthens the transferability of our findings to other vulnerable Andean systems.

This study provides the first interdisciplinary assessment of the Huaper Wetland, combining hydrochemistry, sediment geochemistry, and remote sensing to investigate early-stage degradation in a climatically and ecologically sensitive setting. We hypothesize that anthropogenic salinization, oxygen depletion, and carbonate mineral shifts are progressively weakening the wetland's natural buffering capacity and its ability to retain potential toxic elements such as arsenic and lead. This research aims to elucidate how land-use stressors and climatic variability influence the buffering capacity and water quality of a calcareous wetland in the Central Andes. This is the first integrated study of a high-altitude calcareous wetland in Peru combining hydrochemistry, sediment geochemistry (XRD-EDX), and remote sensing (NDWI). Given that the Huaper Wetland remains unmonitored by national programs despite its ecological vulnerability, it serves as a critical case study for detecting early degradation signals in fragile Andean systems.

2. Methods and materials

2.1. Area of study

The Huaper Wetland is located in the Central Andes, in the Luricocha District, Huanta Province, Ayacucho Region, Peru, at 2353 m above sea level (m a.s.l.) on the eastern slope of the Cachi River valley (12°55′41″ S; 74°17′36″ W). It covers approximately 8.4 ha and provides key ecosystem services, including water regulation, agricultural irrigation, and biodiversity conservation. A steep slope borders the site to the west, with a gentler incline toward the Cachi River in the east. Hydrologically, it is sustained by groundwater

emergence from a central spring, seasonal runoff, and lateral subsurface inflow, with an artificial outflow channel regulating surface discharge.

The climate is subtropical highland, with wet (October–April) and dry (May–September) seasons. During sampling, atmospheric temperatures ranged from 20.3 °C to 28.1 °C, and water temperatures from 20.5 °C to 21.8 °C. Outflow discharge varied from 0.044 m^3/s (March 2023) to 0.026 m^3/s (November 2024), reflecting seasonal dependence on rainfall and recharge. NDWI trends from 2016–2023 show increasing dry-season moisture loss and surface fragmentation. The carbonate-rich substrate and shallow water table make the wetland sensitive to evaporative concentration and recharge variability.

Land use is predominantly agricultural, with ~75 % of households cultivating alfalfa, maize, potatoes, and beans on ~18 ha adjacent to recharge zones. Fertilizers (urea, ammonium nitrate) are typically applied once or twice per season, and irrigation relies on open-channel diversions without protective vegetative buffers. Livestock grazing within the wetland is recurrent. Agricultural intensity increased by ~15 % between 2023 and 2024.

Tourism is informal and unmanaged, mainly between May and August. Field surveys recorded weekend visitor numbers rising from 22 persons in 2023 (Cardenas Morales et al., 2025) to over 30 in 2024 (~36 % increase), with peaks in January–March. Recreational activities include picnics and camping, leaving impacts such as trampling, fire pits, and litter (plastic wrappers, beverage containers). Solid waste accumulation at informal dumping sites increased by ~25 % in 2024 compared to 2023. Waste is generally burned or buried on-site; minor illegal dumping occurs near the wetland's western margin.

Although no active mining exists within the Huaper basin, INGEMMET records indicate inactive concessions in the wider Cachi Valley. The wetland has no formal protection status but aligns with the conservation priorities of Peru's *Estrategia Nacional de Humedales* (MINAM, (2015)). No regular environmental monitoring is implemented by local authorities, and management is community-based without infrastructure for waste collection, signage, or access control.

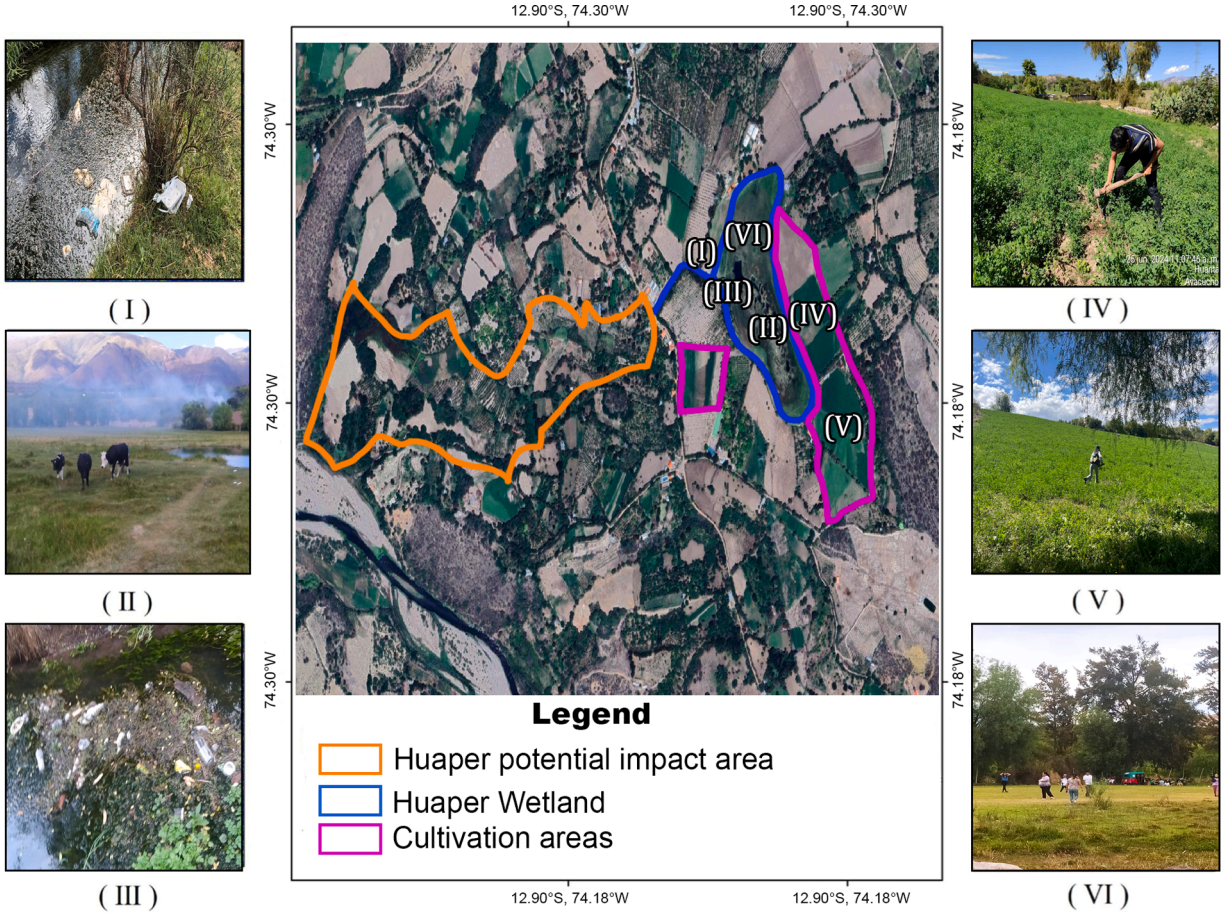

Fig. 1. Google Earth Pro image (2023) showing the boundaries of the Huaper Wetland (blue), surrounding impact area (orange), and zones of active agriculture (magenta). Inset photos I–VI show field evidence of local stressors: (I) localized waste accumulation; (II) grazing within wetland margins; (III) unmanaged solid waste; (IV–V) intensive alfalfa and potato cultivation adjacent to recharge zones; (VI) informal tourism activities. These anthropogenic pressures contribute to the hydrochemical variability observed in the system.

2.2. Sample collection

To evaluate seasonal variability and potential anthropogenic influence, four water sampling campaigns were conducted at two monitoring stations: MH01W-West and MH01W-East. These were strategically selected to capture spatial and temporal hydrochemical differences across the wetland. Sampling dates were March 24, 2023; November 28, 2023; March 27, 2024; and November 30, 2024, corresponding to Austral summer and winter in two consecutive hydrological years. Fig. 1 shows the spatial configuration of the sampling points.

In addition to water monitoring, sediment samples were collected to establish the baseline geochemical and mineralogical profile of the substrate. Seventeen samples were taken on June 14, 2023. These included one at the outlet zone (MH01S-M23), a central reference point (HUAPER CENTRE), and sixteen distributed samples labelled M0 to M15. The sampling points were positioned to encompass multiple depositional zones across the wetland.

Samples were collected using sterilized stainless-steel spatulas, extracting material from the upper 5 cm of sediment. They were stored in sterile zip-lock bags, labelled with GPS coordinates and time of collection, and preserved at −20 °C until laboratory analysis. Due to logistical constraints and the expected short-term stability of sediment composition, sampling was limited to a single campaign during the Austral winter. Full metadata for each sample, including location, date, and sample type, is provided in Table 1.

2.3. Water analysis procedure

The water parameters including pH, electrical conductivity (EC), total dissolved solids (TDS), dissolved oxygen (DO), oxidation-reduction potential (ORP), and temperature were measured in situ using a portable multiparameter meter Hanna HI98494 (Hanna Instruments, Woonsocket, RI, USA). The instrument was calibrated before each campaign according to the manufacturer's specifications to ensure accuracy and consistency across measurements (Hanna Instruments, 2022). This protocol is widely used in aquatic ecosystems, particularly in wetland monitoring (Zhang et al., 2023).

To determine the concentrations of potentially toxic elements (PTE), the water samples were filtered using a vacuum filtration system equipped with 0.45 μm cellulose nitrate membrane filters to remove suspended solids. The filtrates were then acidified to approximately pH 2 with ultrapure nitric acid (HNO_3, Sigma-Aldrich) to stabilize dissolved metals during storage and transport (Vera-Herrera et al., 2022). The acidified samples were stored in polypropylene containers at 4 °C and sent to a certified laboratory (SGS Laboratory, Lima, Peru) for analysis using Inductively Coupled Plasma Mass Spectrometry (ICP-MS). The analytical procedure followed the protocols established by the Peruvian Environmental Quality Standards (ECA-Water), Category 4: Conservation of the Aquatic Environment, as stipulated in Supreme Decree No. 004–2017-MINAM (Ministry of Environment of Peru, (Ministerio del Ambiente, 2017). The ICP-MS method allows high-resolution quantification of trace metals and metalloids, including arsenic (As), cadmium (Cd), lead (Pb), mercury (Hg), chromium (Cr), zinc (Zn), copper (Cu), among others, ensuring robust detection capabilities for hydrochemical assessments in high-altitude ecosystems.

Method detection limits (MDLs) and limits of quantification (LOQs) for all analytes are provided in Supplementary Table MS2. Values below MDL are reported in Table 4 and throughout the text as "<MDL." For descriptive statistics, values <MDL were substituted as MDL/2, following common practice in environmental chemistry (Helsel, 2012). This ensures consistency between reported concentrations and the analytical sensitivity of the ICP-MS method.

2.4. Sediment analysis and characterization

For morphological and granulometric analysis, the samples were dried at 30°C for 24 h to eliminate residual moisture and to prevent carbonization of the organic components. This temperature was also chosen to avoid chemical alteration of the mineral phases. The dried sediment was examined using a Dino-Lite optical microscope, capturing images at a 100 μm scale (×250 magnification). These images were processed to determine the particle size distribution, calculate the mean particle diameter (D) with its standard deviation, and characterize the sediment texture.

To analyse elemental composition, all sediment samples were subjected to Energy Dispersive X-ray Spectroscopy (EDX) using a JEOL JSM-6510LV scanning electron microscope (SEM) coupled with an Oxford Instruments X-Max EDX detector. This setup allowed both qualitative and semi-quantitative identification of major chemical elements. Spectral data were used to estimate the weight percentages of elements such as Ca, O, C, Al, Si, Na, Mg, Fe, K, Ti, P, S, and Mn.

In addition, mineralogical composition was determined using X-ray Diffraction (XRD). Pulverized sediment samples were scanned using a Bruker D8 Advance diffractometer over a 2θ range of 5°–80° with a step size of 0.01°. Diffraction patterns were interpreted by matching them to the ICDD PDF-4 + standard database.

Although trace element quantification via ICP-MS was originally considered, this analysis was not performed on sediment samples due to logistical constraints. Therefore, the geochemical characterization of sediments was based exclusively on EDX and XRD analyses, which provided an integrated overview of the elemental and mineralogical profile of the Huaper Wetland substrate.

2.5. Water Quality Index (WQI) calculation

To assess the Water Quality Index (WQI-PE) of the Huaper wetland, the standards established by Peruvian Environmental Water Quality Standards (ECA-water) office (Method 004–2017-MINAM) were applied (MINAM, 2017). The selected parameters included electrical conductivity, dissolved oxygen (DO), pH, temperature, and concentrations of potentially toxic elements such as arsenic,

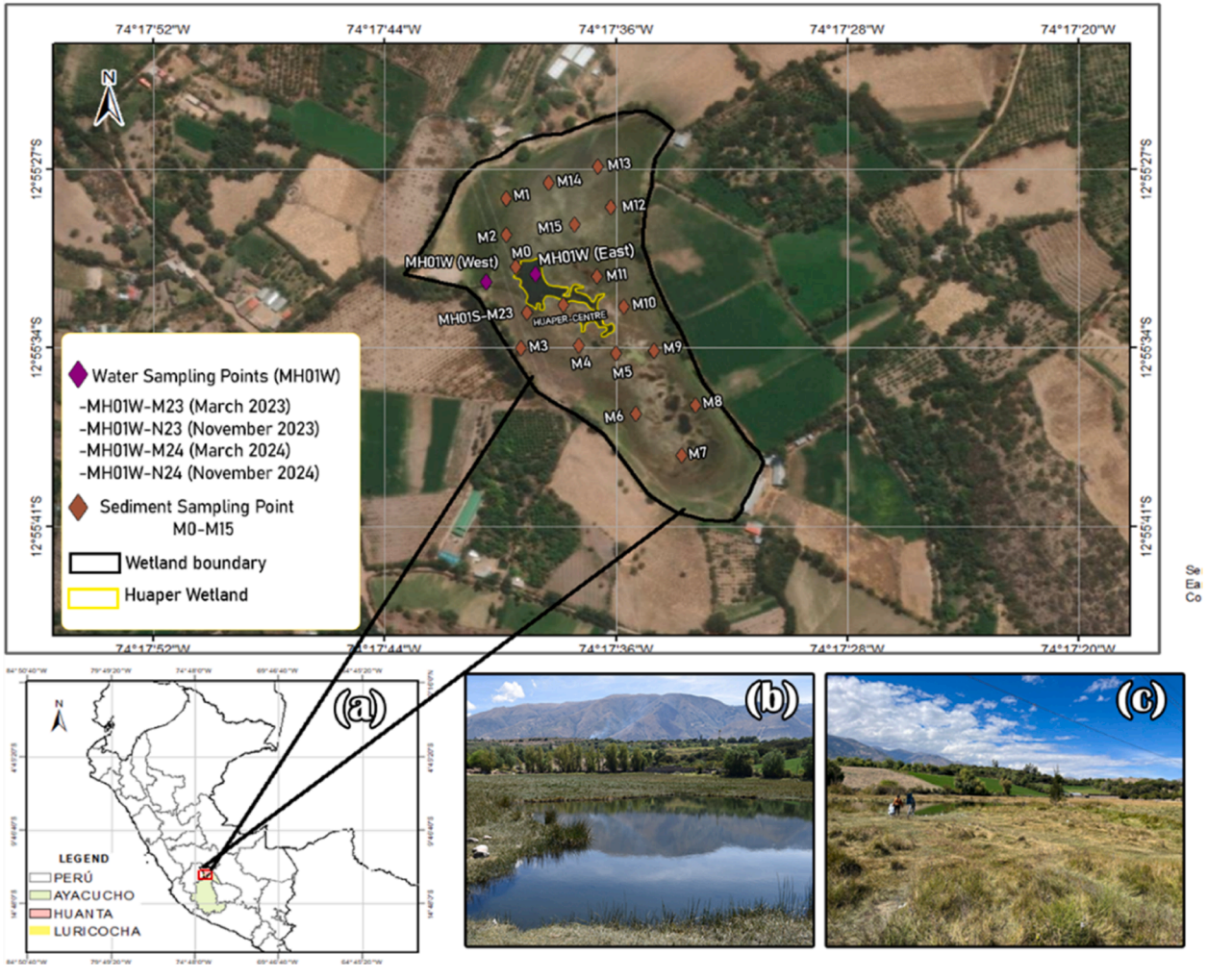

Fig. 2. Geographic Location and Sampling Points of the Huaper Wetland, Huanta, Peru.

Table 1
Description of the samples, geographical coordinates of the sites of collection and date of collection.

Type	Sample	Latitude	Longitude	Sampling Date	Season
Water	MH01W-M23 (West)	12°55'30.71"S	74°17'39.30"W	March 24, 2023	Austral Summer
Water	MH01W-N23 (East)	12°55'31.53"S	74°17'40.62"W	November 28, 2023	Austral Winter
Water	MH01W-M24 (West)	12°55'30.71"S	74°17'39.30"W	March 27, 2024	Austral Summer
Water	MH01W-N24 (East)	12°55'31.53"S	74°17'40.62"W	November 30, 2024	Austral Winter
Sediment	MH01S-M23	12°55'31.06"S	74°17'39.46"W	March 24, 2023	Austral Summer
Sediment	M0	12°55'30.87"S	74°17'39.50"O	June 14, 2023	Austral Winter
Sediment	M1	12°55'28.85"S	74°17'39.17"O	June 14, 2023	Austral Winter
Sediment	M2	12°55'29.19"S	74°17'39.47"O	June 14, 2023	Austral Winter
Sediment	M3	12°55'33.24"S	74°17'39.48"O	June 14, 2023	Austral Winter
Sediment	M4	12°55'33.20"S	74°17'38.41"O	June 14, 2023	Austral Winter
Sediment	M5	12°55'33.65"S	74°17'37.09"O	June 14, 2023	Austral Winter
Sediment	M6	12°55'34.89"S	74°17'37.29"O	June 14, 2023	Austral Winter
Sediment	M7	12°55'38.19"S	74°17'33.64"O	June 14, 2023	Austral Winter
Sediment	M8	12°55'37.01"S	74°17'33.07"O	June 14, 2023	Austral Winter
Sediment	M9	12°55'35.51"S	74°17'34.03"O	June 14, 2023	Austral Winter
Sediment	M10	12°55'34.31"S	74°17'34.75"O	June 14, 2023	Austral Winter
Sediment	M11	12°55'33.54"S	74°17'36.09"O	June 14, 2023	Austral Winter
Sediment	M12	12°55'29.92"S	74°17'35.78"O	June 14, 2023	Austral Winter
Sediment	M13	12°55'27.36"S	74°17'36.07"O	June 14, 2023	Austral Winter
Sediment	M14	12°55'27.31"S	74°17'37.14"O	June 14, 2023	Austral Winter
Sediment	M15	12°55'29.03"S	74°17'37.34"O	June 14, 2023	Austral Winter
Sediment	HUAPER CENTRE	12°55'32.29"S	74°17'37.90"O	June 14, 2023	Austral Winter

cadmium, lead, and zinc. These parameters are essential for evaluating water quality due to their ecological significance and their role as indicators of environmental stressors in high Andean wetlands, particularly concerning anthropogenic activities (Ministerio del Ambiente, 2017; Zhang et al., 2023).

The WQI-PE calculation followed a weighted aggregation approach, where each parameter was assigned a specific weight based on its environmental relevance and permissible limits following the Peruvian regulations. The final index was classified into qualitative categories to facilitate interpretation of the overall water quality status of the wetland. The WQI-PE calculation for the Huaper wetland followed the steps based on the methodology established by the National Water Authority (ANA, Process N.º 084–2020-ANA).

Firstly, to calculate the percentage of parameters that exceed the established ECA-water by using the formula (Scope F1):

$$F1 = \left(\frac{Number\ of\ parameters\ that\ do\ not\ comply}{Total\ number\ of\ parameters\ evaluated}\right) \times 100 \quad (1)$$

This step is crucial for identifying potential exceedances in water quality and assessing regulatory compliance. The regulatory limits for each evaluated parameter are detailed in Table S1 (Supplementary Material), following the Peruvian Environmental Water Quality Standards (ECA) as defined in Decreto Supremo N° 004–2017-MINAM.

Secondly, to determine the proportion of instances in which the evaluated parameters exceed the regulatory limits (Frequency F2):

$$F2 = \left(\frac{Number\ of\ parameters\ that\ do\ not\ comply}{Total\ number\ of\ parameters\ evaluated}\right) \times 100 \quad (2)$$

This step helps identify the recurrence of exceedances at each monitoring station.

Thirdly, to measure the severity of exceedances using the normalized sum of surpluses (Magnitude F3):

$$F3 = \left(\frac{Normalized\ Sum\ of\ Surpluses}{Normalized\ Sum\ of\ Surpluses + 1}\right) \times 100 \quad (3)$$

where the normalized sum of surpluses (NSE) is defined as:

$$\mathrm{NSE} = \frac{\sum \mathrm{Surpluses}}{\mathrm{Total\ data}}$$

Surpluses are calculated as the difference between the observed value and the ECA limit, providing a measure of deviation.

The Environmental Quality Index for Water Resources (ICA-PE) is a numerical representation of water quality. In this study, it is calculated using the standardized parameters established by the Peruvian Environmental Water Quality Standards (ECA-Water). The ICA-PE integrates the extent (F1), frequency (F2), and magnitude (F3) of regulatory exceedances to evaluate environmental condition.

A higher ICA-PE score (closer to 100) indicates better water quality, suggesting that most regulatory standards are met. Conversely, values below 50 imply a critical decline in water quality, meaning the wetland may be affected by excessive contaminants such as heavy metals, excess nutrients (e.g., from fertilizers), or organic waste that depletes oxygen and threatens aquatic life.

In this context, "regulatory standards" refer to official thresholds set by the Ministry of Environment of Peru (MINAM) that define acceptable concentrations of pollutants in water bodies. These thresholds are designed to protect aquatic ecosystems and public health. Exceeding these levels—particularly for toxic elements like arsenic, lead, or cadmium—signals ecological risk and regulatory noncompliance. A "critical decline in water quality," as flagged by ICA-PE scores below 50, reflects a state in which the water no longer meets minimum environmental safety criteria and may be severely impacted by diffuse sources of pollution such as untreated runoff, fertilizers, or solid waste.

The final ICA-PE formula is expressed as:

$$ICA - PE = 100 - \sqrt{\frac{F1^2 + F2^2 + F3^2}{3}} \quad (4)$$

2.6. Normalized Difference Water Index (NDWI) calculation

To assess temporal fluctuations in surface water coverage and hydrological dynamics of the Huaper Wetland, the Normalized Difference Water Index (NDWI) was applied. This geospatial indicator provides insight into seasonal moisture availability and its influence on hydrochemical processes in calcareous wetland systems.

NDWI was calculated using the green and near-infrared (NIR) spectral bands, based on the original method by (McFeeters, 1996):

$$NDWI = \frac{Green - NIR}{Green + NIR}$$

Both bands were obtained from Sentinel-2A and Sentinel-2B satellites at a spatial resolution of 10 m. The selected imagery corresponds to four representative dates: April 2023, November 2023, May 2024, and August 2024, which were chosen to capture

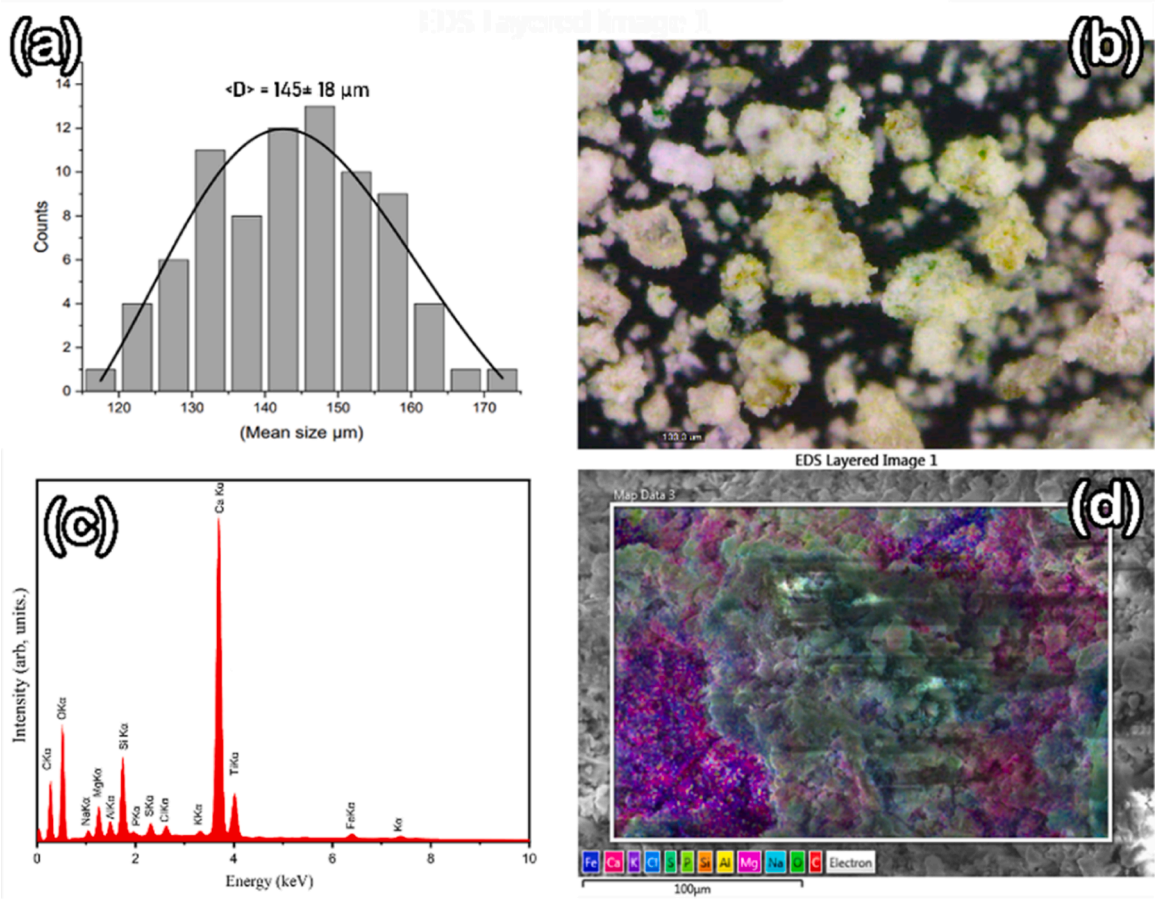

Fig. 3. Morphological and geochemical analysis of a representative sediment sample (M-CENTRE) from the Huaper Wetland. (a) Particle size distribution showing a log-normal profile with a mean diameter of 145 ± 18 µm. (b) Optical micrograph of sediment particles captured using a Dino-Lite microscope at × 250 magnification. (c) EDX spectrum of sample M-CENTRE showing major elemental composition. (d) EDX elemental mapping of the same sample illustrating spatial distribution of Ca, Si, Al, Fe, Mg, Na, and other detected elements.

seasonal variations between wet and dry periods in the Andes.

All images were pre-processed using Sen2Cor in the SNAP software (ESA) for atmospheric correction. This step ensures that radiometric values are consistent and comparable across the different dates.

Subsequently, the NDWI raster outputs were generated using the Raster Calculator tool in ArcGIS Pro 3.2. A threshold value of 0 was used to differentiate water bodies (NDWI $>$ 0) from non-water surfaces (NDWI $<$ 0), following the method proposed by (Xu, 2006).

Finally, Zonal Statistics were applied within the predefined boundary of the Huaper Wetland to extract the mean, minimum, maximum, and standard deviation of NDWI values for each image date. These metrics were used to quantify the surface water coverage and its temporal variation throughout the study period.

Although the NDWI method is widely used to assess surface moisture dynamics, it has known limitations in distinguishing between shallow water, saturated soils, and vegetated wet areas. Additionally, the use of a fixed threshold (NDWI $>$ 0 for water) may lead to misclassification under certain conditions, such as increased turbidity or emergent vegetation. To address this, the NDWI values were interpreted cautiously and complemented with field observations.

NDWI values were extracted using Zonal Statistics within a manually digitized wetland boundary, validated against high-resolution Google Earth imagery to minimize spatial inaccuracies.

3. Results

3.1. Sediment analysis

This section presents the sediments characteristics from the Huaper Wetland using physical and chemical techniques. The objective is to better understand sediment-based retention mechanisms for trace elements and sediment–water interactions.

The particle size analysis revealed mean grain diameters of 133 $\pm$ 14 μm for Sample M1, 152 $\pm$ 8 μm for Sample M2, and 145 $\pm$ 18

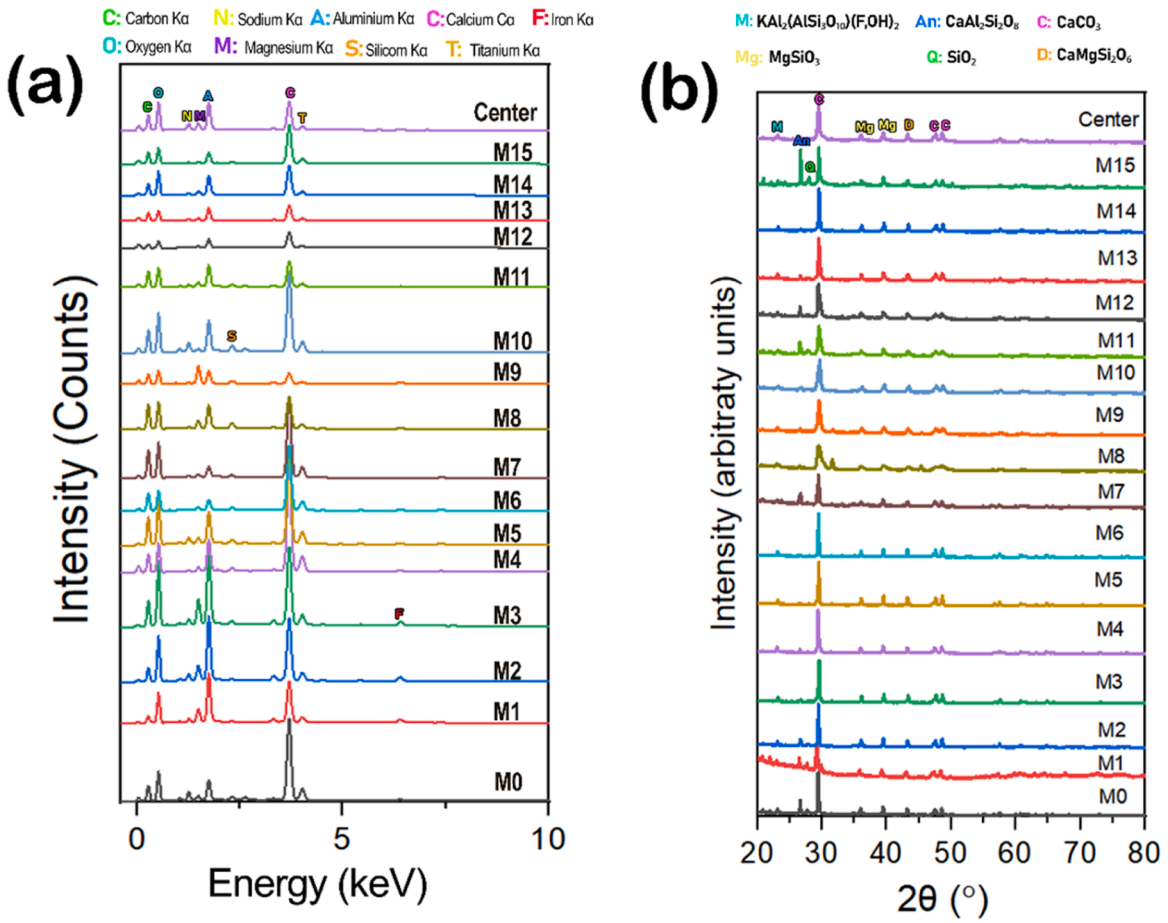

Fig. 4. Geochemical and mineralogical characterization of Huaper Wetland sediments. (a) EDX spectra showing elemental profiles of samples M0–M15, highlighting major elements (Ca, O, C, Si). (b) XRD diffractograms indicating dominant calcite phases and secondary silicates including quartz, diopside, and muscovite.

μm for the M-Centre site (see Fig. 3a, Figure MS2, and Table MS4). According to the Wentworth scale, all samples correspond to the medium to fine sand category. The reported values are derived from log-normal fits to the particle size histograms and indicate broadly consistent granulometric conditions across the wetland. Fig. 3a corresponds exclusively to the M-Centre sample, while granulometric data for M1 and M2 are presented in Supplementary Figure MS2. The distributions follow a log-normal pattern, suggesting well-sorted sediments deposited through fluvial and gravitational processes. The microscopic analysis in Figs. 3a and 3b shows irregular, angular, and highly porous particles, which are typical of low-energy depositional environments with minimal post-depositional transport (Bustamante Domínguez et al., 2012).

These morphological traits enhance the adsorption capacity of the sediments for trace metals such as arsenic (As), lead (Pb) and cadmium (Cd), as reported in previous studies (Silva et al., 2021; Wang et al., 2016). The prevalence of sand-sized particles with sharp edges and porous surfaces is consistent with mechanical weathering and recent sedimentation. These processes are common in high-altitude Andean wetlands characterized by limited hydrodynamics and strong lithological control (Ross, 2023) . The evidence suggests that the Huaper Wetland has low anthropogenic sediment input and functions as an effective geochemical filter.

The elemental and mineralogical composition of all sediment samples (M0–M15) were obtained by using Energy Dispersive X-ray Spectroscopy (EDX) and X-ray Diffraction (XRD), respectively. The results are presented in (Fig. 4a) and Table 2. Calcium (Ca), oxygen (O), and carbon (C) were the dominant elements across all samples, confirming the prevalence of carbonate phases. Calcium content ranged from 11.09 % to 41.80 %, while silicon (Si), magnesium (Mg), and sodium (Na) appeared in lower proportions, particularly in samples M0–M2, where elevated Si aligns with quartz signals. Phosphorus (P), sulphur (S), potassium (K), aluminium (Al), and iron (Fe) were detected at < 3 %, which are consistent with minor silicate and related minerals. Phosphorus and sulphur were detected at levels below 1 %, suggesting minimal organic or anthropogenic enrichment.

XRD results (Fig. 4b, Table 3) confirmed calcite ($CaCO_3$) as the principal mineral phase, with distinct diffraction peaks at $2\theta \approx 29.4°$, 39.4°, and 47.4°. Secondary minerals included quartz (SiO_2), diopside ($CaMgSi_2O_6$), muscovite, anorthite, and clinoenstatite, varying across depth profiles. Quartz was most abundant in surface samples (M0–M2), while silicates were more common in mid-depth layers, suggesting a mix of lithogenic inputs and depositional sorting.

Overall, the abundant presence of calcite supports the classification of the Huaper Wetland as a calcareous system with strong geochemical buffering potential, while the presence of trace silicates indicates heterogeneous provenance.

3.2. Water analysis

Table 4 presents the physicochemical parameters measured in the Huaper Wetland across the four monitoring periods: Austral Summer (March 2023; samples MH-01 (W1) and MH-01 (S)), Austral Winter (November 2023; sample MH-01 (W2)), Austral Summer (March 2024), and Austral Winter (November 2024). The electrical conductivity (EC) values ranged from 866 μS/cm (March 2023) to 944 μS/cm (November 2024), remaining below the Peruvian Environmental Water Quality Standards (ECA-Water) threshold of 1000 μS/cm for lakes and lagoons. The elevated EC observed in November 2023 coincides with the onset of the rainy season, and may be consistent with dry-season mineral accumulation followed by delayed leaching and sediment mobilization, a pattern influenced by groundwater reemergence lag times observed in similar tropical wetland systems (Karimian et al., 2017; Forrest, pers. obs.).

Dissolved oxygen (DO) levels showed notable seasonal variation. The maximum value was 5.71 mg/L in November 2023, exceeding the 5.0 mg/L threshold for aquatic life. However, DO levels dropped below 3.0 mg/L, reaching a minimum of 1.93 mg/L in November 2024, during the dry season. Such reductions are commonly associated with limited vertical mixing, higher evapotranspiration, and lower water renewal rates—patterns observed in similar highland and semi-arid wetlands (Hong et al., 2020).

The pH values ranged from 6.92 to 7.22, remaining within the ECA-Water acceptable range ($\geq$6.5). The neutral pH suggests a buffering system consistent with carbonate-rich environments, where calcium and bicarbonate equilibrium maintain chemical

Table 2
Elemental Composition (in wt%) of Sediments from the Huaper Wetland obtained by EDX analysis (Samples M0–M15).

Sample	C	O	Na	Mg	Al	Si	P	S	K	Ca	Ti	Mn	Fe	Total (wt%)
M0	13.22	35.37	0.46	1.16	4.38	16.4	0.21	0.31	1.54	22.59	0.4	0.14	3.82	100
M1	15.93	35.86	0.64	1.57	3.42	14.31	0.35	1.46	22.74	0.3	0.16	3.22	0.02	100
M2	20.33	36.46	0.35	0.8	3.99	13.35	0.56	1.06	20.21	0.29	0.07	2.5	0.03	100
M3	15.42	30.98	0.38	0.98	7.18	0.12	0.82	42.3	0.19	0.07	1.54	0.01	0	100
M4	21.91	36.97	0.5	1.22	1.12	6.22	0.83	0.32	0.32	29.41	0.13	0.06	0.96	100
M5	20.31	33.14	0.41	1.22	3.68	0.97	0.05	38.35	0.61	0.02	0.87	0.38	0	100
M6	25.73	46.99	0.4	0.7	3.16	0.62	0.12	0.02	19.95	0.22	0.04	2.05	0	100
M7	42.16	39.33	0.63	2.96	8.83	0.17	2.45	1	0.12	0.23	0.04	2.09	0	100
M8	33.19	28.32	0.48	11.27	8.35	2.08	0.18	0.67	1.1	11.05	0.34	0.1	2.86	100
M9	21.59	35.63	0.89	2.18	0.53	6.8	1.5	0.85	0.36	28.98	0.21	0.12	0.35	100
M10	32.67	32.93	0.41	0.88	1.92	9.28	0.98	0.46	0.36	18.55	0.62	0.28	0.64	100
M11	20.09	33.09	0.45	1.1	1.95	10.35	0.69	0.29	0.96	29.5	0.64	0.28	0.64	100
M12	31.4	37.78	0.66	0.59	4.21	6.53	0.12	0.24	0.26	16.89	0.2	0.07	1.05	100
M13	22.09	38.34	0.39	1.39	8.37	5.42	0.3	0.25	0.1	21.65	0.26	0.1	1.35	100
M14	19.02	32.25	0.4	0.73	5.12	8.94	0.17	0.3	0.75	30.44	0.14	0.09	1.65	100
M15	23.15	31.81	0.3	1.92	2.13	8.56	0.16	0.28	0.71	29.16	0.14	0.09	1.58	100

Table 3
Mineralogical Composition of the Huaper Wetland sediments determined by XRD.

Mineral	Chemical Formula	Code ICCD	Samples and %
Calcite	$CaCO_3$	05–0586	M0 (54.4 %), M1 (52.9 %), M2 (57.4 %), M3 (17.6 %), M4 (62.5 %), M5 (23.3 %), M6 (13.5 %), M7 (24.6 %), M8 (29.4 %), M9 (22.9 %), M10 (28.9 %), M11 (43.9 %), M12 (43.1 %), M13 (55.4 %), M14 (19.6 %), M15 (31.9 %), Centre (40.4 %)
Clinoenstatite	$MgSiO_3$	30–0795	M0 (37.6 %), M2 (36.0 %), M3 (74.3 %), M5 (76.7 %), M8 (48.4 %), M9 (40.6 %), M10 (38.3 %), M14 (65.1 %), Centre (6.8 %)
Muscovite	$KAl_2(AlSi_3O_{10})(F, OH)_2$	07–0032	M0 (3.6 %), M1 (6.4 %), M2 (6.6 %),
Anorthite	$CaAl_2Si_2O_8$	41–1486	M7(7.9 %), M11(18.4 %), M15 (25.2 %), Centre (38.0 %)
Quartz	SiO_2	33–1161	M4 (2.8 %),M7 (6.9 %), M9 (0.6 %), M11 (9.8 %), M12 (11.3 %), M13 (3.5 %),M15 (24.1 %)
Diopside	$CaMgSi_2O_6$	23–1024	M1 (40.7 %), M6 (86.5 %), M7 (24.6 %), M8 (22.2 %), M9 (35.8 %), M10 (32.7 %), M11 (46.3 %), M12 (27.2 %), M13 (41.2 %), M14 (15.3 %), M15 (18.7 %), Centre (14.9 %)

Table 4
Summary of the seasonal physicochemical parameters, toxic elements, and WQI-PE for the water samples collected from the Huaper Wetland during March and November 2023 and 2024. Comparative thresholds are based on the Peruvian ECA-Water standards (MINAM, 2017, Category 4: Conservation of the aquatic environment), with WHO (2017) drinking-water guidelines cited as complementary references.

Parameter	Unity	March 2023	November 2023	March 2024	November 2024	Reference (ECA-Water)
Conductivity	µS/cm	866	910	903	944	1000
Dissolved Oxygen (DO)	mg/L	2.64	5.71	1.43	1.93	$\geq$ 5.0
pH	-	6.96	7.02	6.95	7.22	$\geq$ 6.5–9.0
Temperature (T°)	°C	20.48	20.93	20.69	21.81	Δ 3
Arsenic	mg/L	0.0034	0.0033	0.0025	0.0014	0.15
Cadmium	mg/L	0.00012	0.00004	< 0.00003	< 0.00003	0.00025
Chromium	mg/L	< 0.0003	< 0.00080	< 0.0003	< 0.0003	0.011
Copper	mg/L	< 0.00009	0.00098	0.00034	0.0010	0.10
Mercury	mg/L	< 0.00009	< 0.00009	< 0.00009	< 0.00009	0.002
Lead	mg/L	< 0.0006	< 0.0006	< 0.0006	< 0.0006	0.01
Zinc	mg/L	< 0.0026	0.0091	< 0.0026	< 0.0026	0.12
Classification						
Station	F1 (Scope)	F2 (Frequency)	F3 (Amplitude)	ICA-PE	Classification	
March 2023	0.09	0.09	8.8	94.92	Excellent	
November 2023	0.00	0.00	0.00	100.00	Excellent	
March 2024	0.18	0.18	13.79	92.04	Good	
November 2024	0.18	0.18	13.79	92.04	Good	

Values below the method detection limit (MDL) are reported as "<MDL." Values ≥MDL but <LOQ are reported as "<LOQ" using the LOQ value (e.g., Cr <0.0003). Values ≥LOQ are presented with two significant figures, ensuring consistency with analytical accuracy. Detection and quantification limits (MDL and LOQ) for all analytes are detailed in Supplementary Table MS2.

stability. Such neutral to slightly alkaline pH conditions are known to promote the precipitation of certain metals, reducing their mobility in wetland systems (Stottmeister et al., 2006).

Temperature ranged from 20.48 °C (March 2023) to 23.30 °C (March 2024), measured in situ using a Hanna HI98494 multiparameter probe. The increase in temperature during dry seasons may be attributed to elevated solar radiation at high altitudes and corresponds with patterns observed in comparable Andean ecosystems (Lizama-Allende et al., 2021). Higher temperatures are also associated with reduced oxygen solubility, which can amplify seasonal DO depletion.

The analysis of potentially toxic elements in the Huaper Wetland revealed that all monitored heavy metals remained below regulatory thresholds set by the World Health Organization (WHO, 2017) and the Peruvian ECA-Water standards (MINAM, 2017). These results are consistent with the wetland apparent capacity to function as a geochemical barrier, limiting the accumulation of toxic elements through mechanisms such as adsorption onto sediment surfaces, coprecipitation with iron oxides, and mineral precipitation (Buddhawong et al., 2005). Table 4 provides detailed concentrations of these elements across four sampling periods.

Arsenic (As) showed a decreasing trend from 0.0034 mg/L (March 2023) to 0.0014 mg/L (November 2024), well below the ECA-Water limit of 0.15 mg/L (MINAM, 2017) and also below the WHO drinking-water guideline of 0.01 mg/L (WHO, 2017). This trend may reflect progressive As retention via adsorption onto calcareous and porous sediments, as previously observed in Andean wetlands (Contreras et al., 2015). Seasonal fluctuations suggest increased mobilization during wetter periods, likely linked to hydrodynamic reactivation.

Cadmium (Cd) levels remained minimal across all sampling dates. It was detected at 0.00012 mg/L in March 2023 but fell below detection limits (<0.00003 mg/L) thereafter. The strong retention of Cd may be influenced by its affinity for organic matter and clay minerals, supported by the sediment's fine particle content and mineral structure (Kalani et al., 2021).

Chromium (Cr) was only detected at Station 2 in November 2023 (0.00080 mg/L), and was below detection limits in the remaining

samples. This isolated detection, near zones of active agriculture, suggests localized runoff rather than natural mobilization (Stottmeister et al., 2006).

Copper (Cu) concentrations ranged from < 0.00009 mg/L to 0.00102 mg/L, all well below the ECA-Water limit of 0.1 mg/L (MINAM, 2017). The highest value, observed in November 2024, corresponds with increased sediment activity and runoff from agricultural areas. Cu retention is likely enhanced by carbonate precipitation and complexation with dissolved organic matter, consistent with processes found in calcareous sediment environments (Kadlec and Wallace, 2009).

Mercury (Hg) remained undetected (<0.00009 mg/L) throughout the monitoring periods. Given the redox-sensitive nature of mercury mobilization and the buffering capacity of carbonate-rich systems, its absence may reflect stable geochemical conditions (Zhu et al., 2019).

Lead (Pb) concentrations were consistently below detection limits (<0.0006 mg/L), far below the ECA-Water threshold of 0.01 mg/L (MINAM, 2017). Although no temporal trends could be established due to values remaining undetectable, such low concentrations may be associated with strong retention by carbonate sediments and organic matter, as previously observed in highland wetlands (Kalani et al., 2021).

Zinc (Zn) showed a declining trend from 0.026 mg/L to < 0.0026 mg/L across the study period. This decline may be linked to Zn precipitation with carbonate minerals and complexation with organic matter, a process enhanced in calcareous environments (Stottmeister et al., 2006).

These results support the interpretation of the Huaper Wetland as a dynamic but stable system, where the composition and texture of carbonate-rich sediments actively modulate the transport and retention of toxic elements.

Detection limits (MDL) and quantification limits (LOQ) for all monitored elements are detailed in Supplementary Table MS2; values below the MDL are indicated in Table 4 and throughout the text as "<DL". Reported concentrations were harmonized with the analytical accuracy of the method: values at or below MDL are shown as <DL and not quantified further, while values at or above LOQ are presented with two significant figures. This ensures that all reporting aligns with instrument precision and maintains scientific rigor.

3.3. Water Quality Index (WQI-PE)

The Water Quality Index (WQI-PE), calculated using the Canadian Council of Ministers of the Environment (CCME-WQI) method, reveals trends in the water quality of the Huaper Wetland. The values indicate "excellent" water quality at Station 1 on March 24th, 2023 (Austral Summer), and Station 2 on November 28th, 2023 (Austral Winter), with scores of 94.92 and 100.00, respectively. These results suggest that water parameters meet quality standards for aquatic ecosystems in Category E1 (Lakes and Lagoons) according to Peruvian ECA-Water regulation (MINAM, 2017, Category 4: Conservation of aquatic environment) and are also consistent with WHO drinking-water guidelines (WHO, 2017). The water in these stations is suitable for conservation purposes without requiring additional treatment, aligning with previous studies on healthy high-Andean wetlands (Zhu et al.,2019). (See Table MS1 in the supplemental material).

During the Austral Summer of March 2024, the WQI-PE score was 92.04, classifying the water as "good." Although still within a favorable range, this slight decrease from previous values suggests early signs of degradation. The decline in dissolved oxygen (1.43 mg/L; Table 4) and the rise in water temperature (20.69°C) may be related to seasonal variation and localized human activity. While nearby infrastructure is sparse, isolated sanitation discharges or agricultural runoff may contribute to observed changes, warranting further investigation. Similar patterns have been reported in Andean and Asian wetlands where reduced DO is linked to limited water renewal and biochemical demand (Pham, 2020).

November 30th, 2024 (Austral Winter) also recorded a WQI-PE score of 92.04, maintaining a "good" classification. These results may be influenced by seasonal factors, such as lower recharge during dry periods and proximity to human-impacted areas. Although water quality remained within permissible limits, the drop in dissolved oxygen (DO = 1.93 mg/L) to near-critical levels highlights the need for continuous monitoring, as oxygen depletion could alter metal mobility and ecosystem stability (Kadlec and Wallace, 2009).

These fluctuations align with the broader hydrochemical dynamics described for calcareous wetlands, where carbonate buffering systems can regulate pH and facilitate metal retention, particularly under varying redox conditions (Stottmeister et al., 2006). The stable pH and decreasing concentrations of metals such as As, Zn, and Cd also support the idea that the Huaper Wetland acts as a geochemical buffer, consistent with findings from sediment análisis.

3.4. Cation and anion analysis

The cation and anion analysis revealed seasonal variations that underscore the hydrogeochemical complexity of the Huaper Wetland. Fig. 4 presents the Piper diagram, plotted using the anion and cation values detailed in Table MS3. The key parameters analysed include calcium, magnesium, sodium, bicarbonate, sulphate, nitrate, and chloride, which collectively characterize the ionic composition and mineralogical influence on the aquatic environment.

Calcium (Ca) and magnesium (Mg) concentrations ranged from 6.16 to 7.25 meq/L and 1.42–1.83 meq/L, respectively, contributing to moderate water hardness (37.9–45.5 ppm). These values fall within the Peruvian ECA-Water thresholds for surface water (75 mg/L for Ca, 50 mg/L for Mg), as established by ECA-Agua (MINAM, 2017). The elevated presence of calcium aligns with the dominance of carbonate minerals in the sediments (as previously discussed), confirming the calcareous nature of the wetland. These results are consistent with prior studies in wetlands influenced by limestone-bearing lithologies (Roman-Ross et al., 2006).

The pH ranged from 6.92 to 7.22, indicating nearly neutral to slightly acidic conditions. This contrasts with the expected slight

alkalinity of carbonate-buffered systems, suggesting local geochemical variability. Nonetheless, these values may still support carbonate interactions and partial buffering capacity, as reflected in both water and sediment geochemistry (Roman-Ross et al., 2006; Piper, 1944).

Sodium (Na) concentrations ranged from 33.82 to 44.18 mg/L, exceeding the WHO (2017) guideline of 20 mg/L for drinking water. Although the Peruvian ECA-Water does not specify a sodium threshold, these elevated values may indicate salt leaching or wastewater intrusion, particularly in light of the region's geomorphological and anthropogenic context. Nitrate (NO_3^-) levels fluctuated between 2.43 and 8.09 mg/L. While they remain below the WHO limit of 10 mg/L, the November 2023 value exceeded the Peruvian ECA-Agua (MINAM, 2008) threshold of 7 mg/L, potentially signaling agricultural runoff or domestic wastewater inputs.

Sulphate (SO_4^{2-}) concentrations ranged from 53.61 to 72.25 mg/L, well below the 250 mg/L limit set by WHO (2017) and (U.S. Environmental Protection Agency EPA, 2022). The presence of sulfate is likely due to natural leaching of sulfur-rich lithologies, reflecting patterns typical of highland carbonate terrains (Naser et al., 2017).

Chloride (Cl^-) concentrations were relatively stable (38–51 mg/L), remaining well below the WHO guideline of 250 mg/L. These values suggest limited salinization and minimal urban discharge, supporting the relatively pristine condition of the wetland despite external pressures.

Bicarbonate (HCO_3^-) levels ranged between 394.55 and 488.31 mg/L, confirming the dominance of carbonate buffering in the aquatic chemistry. Combined with the observed pH and hardness, these values reinforce the geochemical influence of calcareous mineral weathering.

The Piper diagram (Fig. 5) reveals that all samples collected in both the 2023 and 2024 summer and winter campaigns cluster in the lower left quadrant of the central diamond, reflecting dominance of bicarbonate in the anion triangle and calcium and magnesium in the cation triangle. According to hydrochemical facies classification, the Huaper Wetland water corresponds to the calcium-magnesium-bicarbonate type. These facies are characteristic of carbonate-rich environments influenced by sedimentary rocks and are indicative of carbonate weathering with minimal evidence of salinity intrusion. The consistency in the spatial distribution of samples across seasons supports the hypothesis of a hydrogeochemical system predominantly influenced by natural geochemical

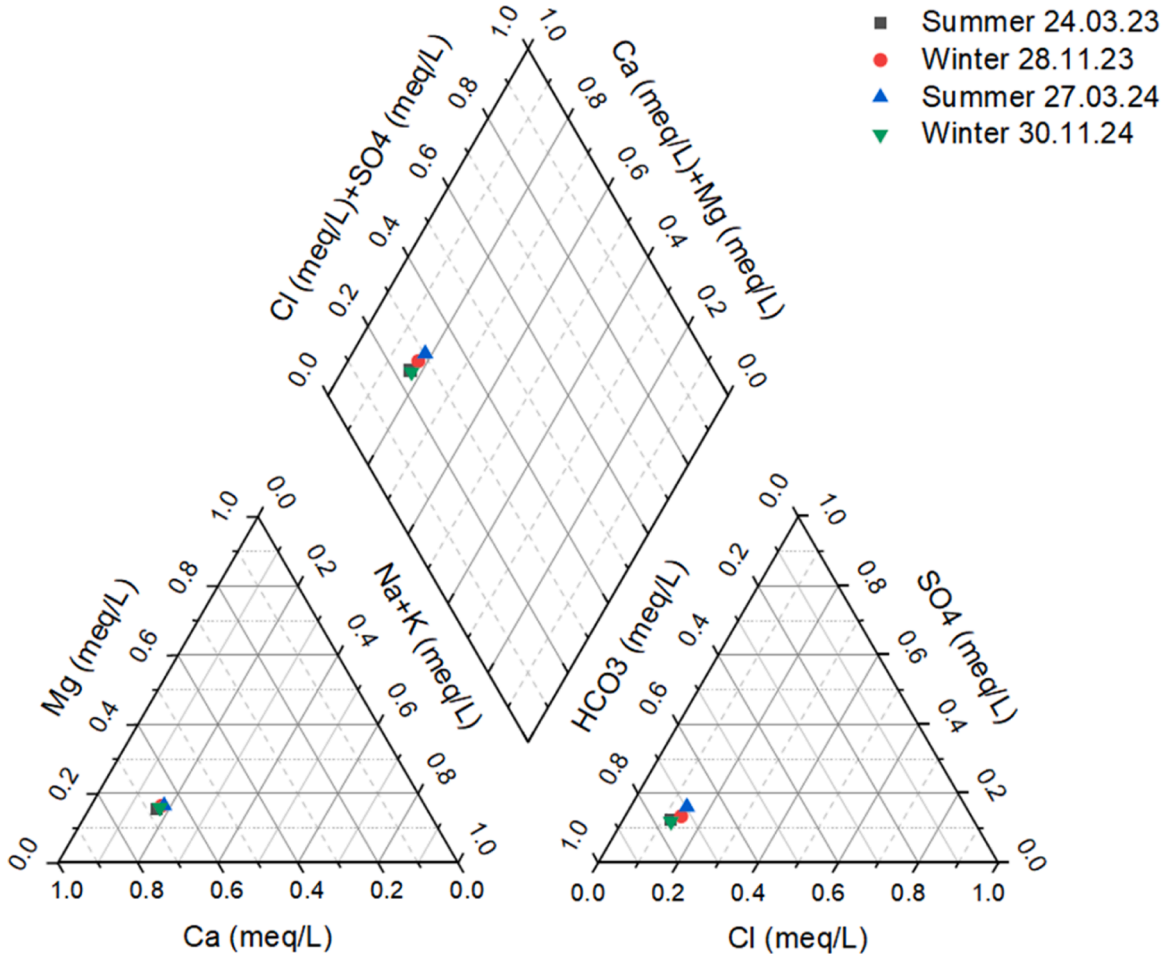

Fig. 5. Piper diagram showing the hydrochemical facies of the Huaper Wetland based on seasonal variations in major cations and anions.

sources (Piper, 1944;Domenico and Schwartz, 1998) .

3.5. NDWI analysis for the Huaper wetland

The Normalized Difference Water Index (NDWI) analysis revealed consistent spatiotemporal changes in water availability in the Huaper Wetland from 2016 to 2023. Satellite-derived NDWI values were extracted for each year using Sentinel-2 imagery to monitor seasonal and interannual variability in surface moisture.

Annual mean NDWI values ranged from –0.3592 in 2016 to a minimum of –0.4699 in 2017, indicating a pronounced moisture deficit in that year. Partial recovery occurred during 2018–2019 (mean NDWI: –0.3784), followed by a period of relative stability through 2020–2021. However, a renewed decline was observed in 2022 (–0.3932), with a modest rebound in 2023 (–0.3759), See Figure MS1.

The highest standard deviation (STD = 0.0716) was recorded in 2017, suggesting spatial heterogeneity in water distribution during the driest year. Between 2019 and 2021, NDWI variability decreased, coinciding with more stable hydrological conditions. The increasing spread in 2022–2023 reflects renewed fluctuations in water coverage, potentially linked to external hydrometeorological factors.

All NDWI values remained consistently negative, indicating low reflectance from open water surfaces and suggesting limited water cover or dominance of saturated soils and emergent vegetation. These negative values align with findings from other Andean wetlands under seasonal stress, and are particularly consistent with calcic wetlands, where evapotranspiration and shallow hydrology result in intermittent moisture exposure of carbonate-rich substrates. (Fig. 6).

4. Discussion

The detection of calcite as the dominant mineral phase, along with secondary silicates such as muscovite and diopside in the sediments of the Huaper Wetland, indicates its potential to buffer pH and to immobilize trace metals through adsorption, co-precipitation, and surface complexation. Similarly, the calcium levels in the sediments (ranging from 11.09 % to 41.8 %), together with the elevated bicarbonate concentrations in the water (394–488 mg/L), confirm its buffering role. Prior research indicates that calcite surfaces, particularly along the (104) crystallographic plane, have high affinity for metals like arsenic and lead, especially under mildly alkaline conditions (Roman-Ross et al., 2006;Sdiri et al., 2012), which matches the pH range observed in Huaper (6.92–7.22).

This buffering function, however, is sensitive to geochemical disruptions. The seasonal drop in dissolved oxygen, at times below 2 mg/L, may create reducing conditions that destabilize carbonate-metal associations and potentially lead to the remobilization of adsorbed contaminants (Luther and Church, 1988; Islam et al., 2004). In parallel, the silicate minerals detected by XRD, such as diopside, clinoenstatite, and anorthite, may also influence ion exchange dynamics and sediment surface reactivity, either enhancing or competing with calcite's capacity to retain metals (Zhao et al., 2020; De Los Santos Valladares et al., 2022).

The geochemical balance suggested by the high calcite and bicarbonate levels appears robust, yet not immune to stress. Although seasonal shifts in arsenic and lead concentrations remain within regulatory limits (MINAM, 2017; WHO, 2017), they are near their thresholds and indicate that the system is susceptible to change. In this context, continuous assessment of trace-level contaminants and evaluation of calcite's retention performance is important in systems exposed to fluctuating hydrochemical conditions (Wang et al., 2016; Laur et al., 2020). Integrating these measurements with spatial-temporal indicators such as NDWI enhances our understanding of wetland vulnerability and contributes to building a framework for future geochemical risk assessments.

The elemental composition of the sediments revealed notable variability in Na levels, reaching up to 0.89 % in certain points. This heterogeneity, along with seasonal increases in electrical conductivity, suggests ongoing salinization processes, particularly during the dry season, which is characterized by limited recharge and elevated evaporation. This phenomenon has also been documented in other high-altitude Andean wetlands exposed to natural weathering and anthropogenic inputs (Carrasco Baquero et al., 2023; Shammi et al., 2019).

The detection of nitratine ($NaNO_3$) supports the hypothesis of agrochemical contamination linked to fertilizers used in nearby cultivated areas. In Andean calcareous soils, interactions with sodium can influence nutrient availability (De Los Santos Valladares et al., 2022).

In the broader context of the Huanta micro-watershed, land use practices combine both agricultural and historical mining pressures. Although no active extraction is currently taking place near the wetland, legacy mining concessions persist in the upper recharge zones of the watershed, while irrigated agriculture dominates the lower slopes surrounding Huaper. This spatial overlap suggests a potential interaction between residual geogenic contamination and diffuse agricultural inputs. For example, fertilizers used in nearby fields may enhance leaching and weathering of natural arsenic-bearing minerals upstream, particularly during the rainy season. Once mobilized, these trace elements can migrate laterally or vertically toward the wetland through shallow groundwater flows or surface runoff. Therefore, rather than acting in isolation, mining and agriculture may jointly influence the hydrochemical balance of the wetland by increasing sodium inputs, altering redox conditions, and weakening the sorptive capacity of calcite. This dual-pressure scenario supports the need for integrated catchment-scale management strategies that address both historical and ongoing anthropogenic stressors.

Excess sodium also has geochemical implications: adsorption studies on carbonate substrates show that Na^+ can displace metals such as As and Pb adsorbed onto calcite surfaces, reducing retention capacity under saline conditions (Baloch et al., 2022). Moreover, research on precipitation and calcite complexes indicates that sodium promotes ionic competition, weakening metal fixation (Roman-Ross et al., 2008).

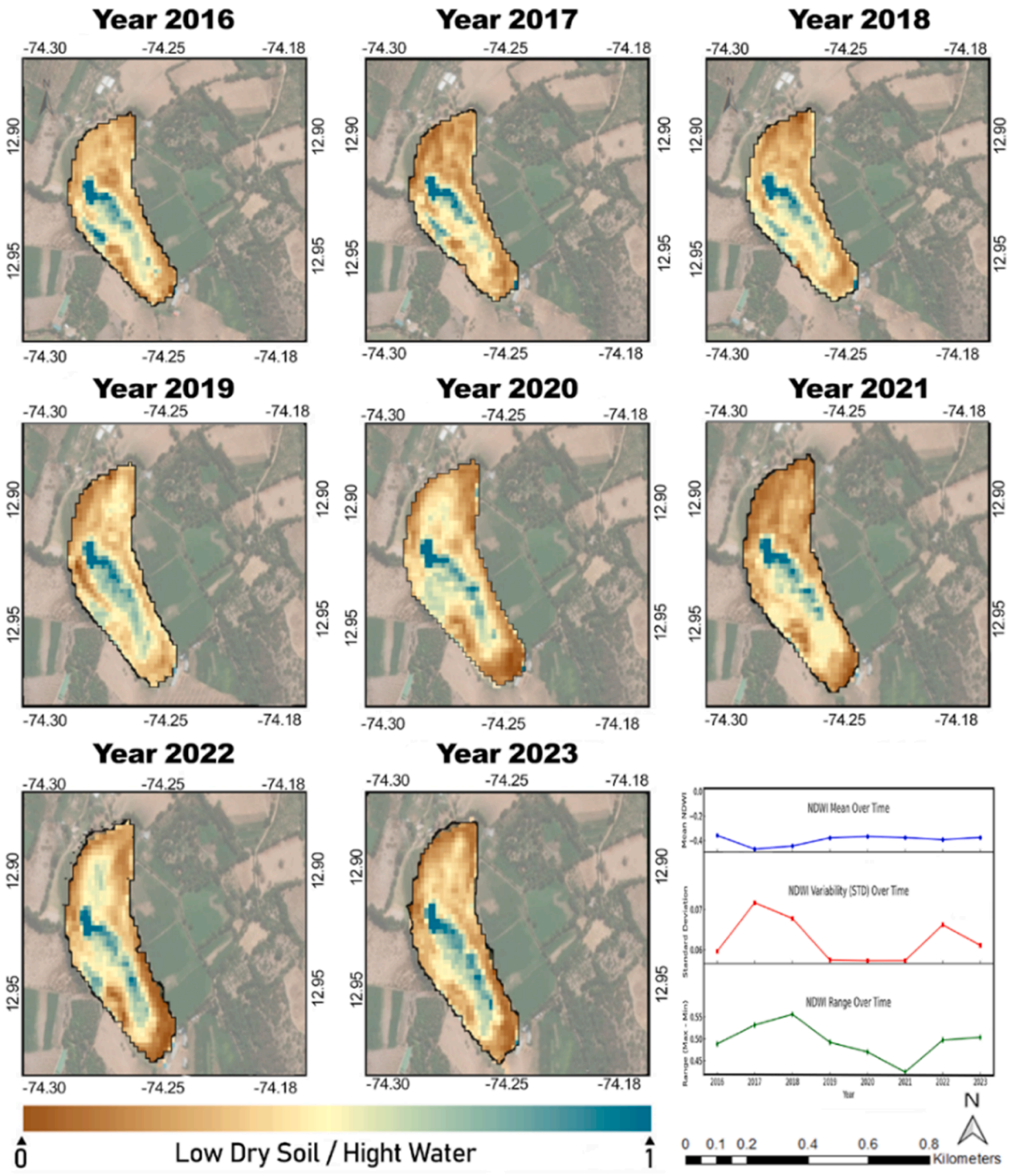

Fig. 6. Temporal NDWI Variation in the Huaper Wetland, Peru, during the years 2016–2023.

Therefore, the interaction between Na^+ and calcite may affect both pH stability and metal retention dynamics within the Huaper Wetland. While calcite can moderately buffer salinity through ion exchange or co-precipitation, persistent sodium accumulation could compromise this equilibrium. Under elevated Na conditions, calcite becomes less effective at sequestering metals, which may explain the seasonal variability observed in As, Pb, Zn, and Cd concentrations. This pattern highlights the importance of monitoring sodium not only as a salinization indicator but also as a potential destabilizing factor in the wetland's geochemical functionality.

Finally, As concentrations remain below regulatory limits but near critical thresholds, and their association with Na further reinforces the need to evaluate local geology. Outcrops of shale and calcareous sandstone in the upper basin, which are part of the broader Huanta micro-watershed, may contain naturally occurring arsenic bound in sedimentary mineral phases, as has been reported in similar Andean systems (for example, in Estero Derecho Wetland, Chile; Oyarzún and Oyarzún, 2011; Romero et al., 2003).

Although no active mining operations have been identified in the immediate vicinity of the Huaper Wetland, recent regional assessments reveal that upstream recharge zones contain legacy mining concessions and arsenic-bearing lithologies (Cardenas Morales et al., 2025). These formations can act as geogenic sources of trace elements. Under undisturbed conditions, arsenic is typically immobile. However, seasonal redox fluctuations, such as the drops in dissolved oxygen observed during dry periods, may favor the reductive dissolution of arsenic-bearing minerals, releasing arsenic into porewater and shallow groundwater. At the same time, increasing sodium concentrations can promote arsenic desorption through ionic competition, weakening its association with calcite and other sediment surfaces. This process has been described in carbonate-rich systems where salinization reduces the retention capacity for trace metals (Roman-Ross et al., 2008; Baloch et al., 2022).

In agricultural contexts, the use of nitrogen-based fertilizers can exacerbate this dynamic by enhancing soil weathering and stimulating leaching. Combined with topographically driven recharge, these diffuse agrochemical inputs may contribute to the mobilization of arsenic toward the wetland. Taken together, these factors support a scenario in which naturally occurring arsenic is mobilized not by direct industrial discharge but through land use–induced geochemical destabilization. Future studies should include comparative soil and groundwater analysis to quantify the role of geogenic and land use interactions in trace element dynamics.

The NDWI analysis between 2016 and 2023 revealed marked interannual variability in surface moisture, highlighting the hydrological fragility of the Huaper Wetland. The lowest NDWI value, recorded in 2017 (−0.4699), corresponds to a year of acute climatic irregularity and suggests a significant reduction in water availability. Although partial recovery was observed in 2018 and 2019, the persistently negative NDWI values and increasing standard deviation indicate a sustained decline in moisture retention and the formation of localized desiccation zones. These spatial fluctuations may reflect the combined effect of topographic gradients and land-use dynamics in the surrounding area. The fragmentation of water coverage is consistent with the initial stages of hydroecological deterioration observed in other Andean wetlands, such as those reported in the high-altitude regions of Bolivia, Chile, and Ecuador, where reduced surface moisture and increased salinity were linked to both climatic variability and land-use pressures (Wetlands, 2024; Duhalde et al., 2024; Carrasco Baquero et al., 2023).

Note that NDWI is sensitive to changes in surface transparency, which can be related to the presence of suspended carbonates or sediments. This in turn can modulate reflectance and thus obscure subtle hydrological trends. In this context, NDWI should not be interpreted as a purely hydrological proxy but rather as an integrative signal that may capture both physical and geochemical transformations within the wetland (Duhalde et al., 2024). The increasing variability of NDWI during dry periods may also be linked to reduced vertical water exchange and declining recharge. These conditions are particularly relevant for calcareous wetlands, where shallow water tables and mineral-rich substrates are especially vulnerable to climatic anomalies. If sustained, these patterns could compromise the buffering capacity of the system, reducing its ability to regulate pH and immobilize metals.

From an ecological perspective, the co-occurrence of salinization, declining dissolved oxygen, and moisture fragmentation suggest a transition toward a less resilient wetland state. Seasonal drops in dissolved oxygen below 2 mg/L, particularly during the 2024 dry season, indicate the development of hypoxic conditions that may impair aerobic microbial processes, aquatic respiration, and trophic balance. These patterns are not isolated but have been increasingly reported in other high-altitude wetland systems worldwide. For instance, similar processes have been documented in Estero Derecho, a high-Andean wetland located in the Elqui River basin in semi-arid Chile (Duhalde et al., 2024), the wetlands of the Ecuadorian Andes (Carrasco Baquero et al., 2023), and highland peatlands in Bolivia and Argentina (Wetlands, 2024) .

Many of these changes, such as increased evaporative concentration, reduced recharge during dry seasons, and oxygen depletion, are being amplified by ongoing climate change, which alters precipitation regimes, intensifies droughts, and elevates temperatures in mountain regions (Buytaert et al., 2011; Cuesta et al., 2019). These climatic shifts exacerbate water loss, accelerate salinization, and compress ecological thresholds in fragile alpine systems. In the case of the Huaper Wetland, the intensification of dry season stressors and rising ionic loads reflect regional expressions of these global climatic pressures. This trend aligns with global concerns about the future viability of high-altitude wetlands as climate buffers and biodiversity hotspots (Convention on Biological Diversity, 2021).

Additionally, such stressors can interact with geogenic contamination, especially in legacy mining regions of the Peruvian Andes, where altered hydrodynamics mobilize naturally occurring toxic elements such as arsenic and lead (Castillo Corzo et al., 2022; Castillo Corzo et al., 2025; Pham, 2020). Therefore, the observed degradation signals at Huaper are part of a broader pattern increasingly associated with climate-driven ecological destabilization in mountain wetlands across the Andes and other alpine regions.

The elevated sodium concentrations in both water and sediments promote gradual salinization, potentially driven by evaporative losses and agricultural runoff. This increase in ions can affect plant water uptake, degrade soil structure, and shift the system toward dominance by halotolerant taxa. Over time, these conditions may compromise the biological integrity of the Huaper Wetland, especially for species adapted to low-conductivity and oxygen-rich environments. Furthermore, the interaction between sodium and carbonate minerals is geochemically significant. Under sodium-enriched conditions, the adsorption capacity of calcite for PTE is reduced, particularly under scenarios of ionic competition and pH fluctuations. This effect limits the wetland's natural filtration capacity and may lead to episodic remobilization of contaminants during redox changes. Given the high calcium and bicarbonate content observed in the system, preserving these chemical conditions is essential to ensure continued metal retention and buffering efficiency.

The integration of multiple methodological approaches, including hydrochemical monitoring, spectroscopic sediment analysis, trace element quantification, and multi-temporal NDWI assessment performed here, provided a comprehensive understanding of the Huaper Wetland's current condition. The identification of calcite as the dominant mineral, along with elevated bicarbonate levels,

reinforces the classification of this system as calcareous and supports its function as a natural geochemical barrier. However, the observed decline in oxygen levels, gradual salinization, and hydrological fragmentation highlight incipient degradation patterns that require attention.

The Water Quality Index (WQI-PE) classified two stations as "excellent" and two as "good", indicating early-stage alteration rather than critical deterioration. Nevertheless, the presence of geochemical stressors and subtle shifts in water chemistry suggests that the system is approaching a functional threshold. Similarly, the NDWI analysis, when interpreted alongside hydrochemical indicators, revealed progressive moisture loss and increased spatial variability, highlighting the need for integrated monitoring frameworks. Therefore, future conservation efforts should focus on protecting the recharge areas of the wetland, reducing nutrient and agrochemical inputs from surrounding farms, and maintaining the chemical stability of the calcareous substrate. Long-term monitoring of sodium dynamics, oxygen fluctuations, and mineral stability is essential to preserve the ecological integrity and buffering capacity of the Huaper Wetland. Evidence from other Peruvian sites shows that anthropogenic contamination, particularly from agriculture and legacy mining, can alter the mineralogy and trace metal retention of soils (Bustamante Domínguez et al., 2012).

5. Conclusion

A detailed assessment of the Huaper Wetland was conducted by integrating hydrochemical monitoring, geochemical sediment analysis, and remote sensing evaluation. The Water Quality Index (WQI-PE) indicates that most sampling sites maintain excellent to good water quality, aligning with national and international standards. However, seasonal declines in dissolved oxygen and slight increases in conductivity suggest early-stage hydrochemical imbalances, potentially influenced by moderate anthropogenic pressures and natural recharge fluctuations. The sediment composition confirmed the dominance of calcite and magnesium-calcite, typical of carbonate-rich environments with high buffering potential. This mineralogical configuration supports pH stability and favours the retention of potentially toxic elements (PTEs). Nevertheless, the detection of sodium, borates, and nitrates, along with evidence of oxygen depletion, suggests diffuse inputs that are likely related to agricultural runoff or atmospheric deposition. Thus, this study presents the first geochemical and hydrochemical baseline for the Huaper Wetland, yet it is not without limitations.

The findings are based on four seasonal sampling campaigns across two hydrological years; however, they may not capture extreme interannual variability or long-term trends. Furthermore, the study did not evaluate microbial activity or biological indicators that may influence redox processes. Spatially, the sampling density may limit resolution of fine-scale gradients in sediment chemistry or groundwater interactions. Future studies should prioritize multiyear monitoring programs to detect longer-term shifts, explore microbial and isotopic indicators of redox evolution, and assess land-use change impacts using finer-resolution remote sensing. Comparative studies with other calcareous wetlands in the Andes would also help contextualize the findings and assess regional generalizability. Despite these limitations, the approach presented here demonstrates the value of combining hydrochemical data, sediment mineralogy, and NDWI time series to evaluate high-altitude calcareous wetland dynamics. The results provide actionable insights for land-use regulation, salinity control, and conservation planning. This work contributes to broader hydrological efforts aimed at maintaining water security and ecosystem resilience in Andean regions increasingly affected by climatic and anthropogenic stressors.

CRediT authorship contribution statement

B.K. Cardenas Morales, L. De Los Santos Valladares, and J. Forrest contributed to data acquisition, methodology, formal analysis, and data curation. Conceptualization, validation, interpretation, and visualization were carried out by B.K. Cardenas Morales, W.V. Castro Aponte, B. La Torre, H.E. Sanchez Cornejo, J. Johncon Coyip, P. Byrne, T.T. Nguyen, C.H.W. Barnes, and L. De Los Santos Valladares. All authors contributed to writing—original draft preparation and writing—review and editing.

Declaration of Competing Interest

The authors declare no competing interest

Acknowledgements

This work was supported by a Collaboration Agreement between the Universidad Nacional Autonoma de Huanta (Peru) and the University of Cambridge (UK), Contract Number G117323. H. Sanchez thanks the Peruvian Council of Science and Technology CONCYTEC for financial support through grant No. PE501087367–2024-PROCIENCIA.

Appendix A. Supporting information

Supplementary data associated with this article can be found in the online version at doi:10.1016/j.ejrh.2025.102767.

Data availability

Data will be made available on request.

References

Baloch, M.Y.J., Zhang, W., Zhang, D., Al Shoumik, B.A., Iqbal, J., Li, S., Chai, J., Farooq, M.A., Parkash, A., 2022. Evolution mechanism of arsenic enrichment in groundwater and associated health risks in Southern punjab, Pakistan. Int. J. Environ. Res. Public Health 19 (20), 13325. https://doi.org/10.3390/ijerph192013325.

Buddhawong, S., Kuschk, P., Mattusch, J., et al., 2005. Removal of arsenic and zinc using different laboratory model wetland systems. Environ. Sci. Eng. https://doi.org/10.1002/elsc.200520076.

Bustamante Domínguez, J., Fabián Salvador, L., De Los Santos Valladares, C.H.W.Barnes, Yutaka, Majima, 2012. Mössbauer study of contamined soils by industrial activity in paramonga city, region Lima provinces, Peru. Hyperfine Interact. 211, 147–152. https://doi.org/10.1007/s10751-012-0591-x.

Buytaert, W., Cuesta-Camacho, F., & Tobón, C. (2011). Potential impacts of climate change on the environmental services of humid tropical alpine regions.

Cardenas Morales, B.K., Oré Gálvez, S.F., Castro Aponte, W.V., Aguilar Ozejo, A., Ñaupari Molina, R., Huayhua Lévano, F.G., Mendoza Colos, M., 2025. Integrating education and conservation: a case study of the huaper wetland. Front. Psychol. 16. https://doi.org/10.3389/fpsyg.2025.1517653.

Carrasco Baquero, J.C., Caballero Serrano, V.L., Romero Cañizares, F., Carrasco López, D.C., León Gualán, D.A., Vieira Lanero, R., Cobo-Gradín, F., 2023. Water quality determination using soil and vegetation communities in the wetlands of the Andes of Ecuador. Land 12 (8), 1586. https://doi.org/10.3390/land12081586.

Castillo Corzo, M.A., Peña Rodriguez, V.A., Manrique Nugent, M.A., Villarreyes Peña, E.G., Byrne, P., Gonzalez Gonzalez, J.C., Patiño Camargo, G., Barnes, C.H.W., Sanchez Ortiz, J.F., Saldaña Tovar, J., De Los Santos Valladares, L., 2025. Potentially toxic elements and radionuclides contamination in soils from teh vicinity o fan ancient Mercury mine in huancavelica, Peru. Soil Sci. Annu. 76 (2), 204389. https://doi.org/10.37501/soilsa/204389.

Contreras, M.T., Müllendorff, D., & Pastén, P. (2015). Potential accumulation of contaminated sediments in a reservoir of a high-Andean watershed: Morphodynamic connections with geochemical processes.

Convention on Biological Diversity (CBD). (2021). The state of mountain biodiversity and ecosystem services. https://www.cbd.int.

Corzo, M.A.Castillo, Borja-Castro, L.E., Valladares, L.De. Los Santos, Gonzalez, J.C., Medina Medina, J., Quinde, A.Trujillo, Barnes, C.H.W., Peña Rodríguez, V.A., 2022. Magnetic, structural and Mössbauer study of soils from an ancient mining area in huancavelica – Peru. Hyperfine Interact. 243, 3. https://doi.org/10.1007/s10751-021-01786-8.

Cuesta, F., Peralvo, M., Muriel, P., & Viña, A. (2019). Ecosystem-based adaptation for high Andean communities: Linking science, policy, and practice.

Dangles, O., Rabatel, A., Kraemer, M., Zeballos, G., Soruco, A., 2017. Ecosystem sentinels for climate change: present and future variability of high-Andean biodiversity in a changing world. PLOS ONE 12 (5), e0175814. https://doi.org/10.1371/journal.pone.0175814.

Dinsa, T.T., Gemeda, D.O., 2019. The role of wetlands for climate change mitigation and biodiversity conservation. J. Appl. Sci. Environ. Manag. 23 (7), 1271–1275. https://doi.org/10.4314/jasem.v23i7.16.

Domenico, P.A., Schwartz, F.W., 1998. Physical and Chemical Hydrogeology, 2nd ed. Wiley.

Dubuc, A., Waltham, N., Malerba, M., Sheaves, M., 2017. Extreme dissolved oxygen variability in urbanised tropical wetlands: the need for detailed monitoring to protect nursery ground values. Estuar. Coast. Shelf Sci. 198, 163–171. https://doi.org/10.1016/j.ecss.2017.09.014.

Duhalde, D., Cortés, J., Arumí, J.-L., Boll, J., Oyarzún, R., 2024. Exploring the behavior of the high-Andean wetlands in the semi-arid zone of Chile: the influence of precipitation and temperature variability on vegetation cover and water quality. Water 16 (24), 3682. https://doi.org/10.3390/w16243682.

Erwin, K.L., 2009. Wetlands and global climate change: the role of wetland restoration in a changing world. Wetl. Ecol. Manag. 17 (1), 71–84. https://doi.org/10.1007/s11273-008-9119-1.

Flower, H., Rains, M., Taşcı, Y., Zhang, J.-Z., Trout, K., Lewis, D., Dalton, R., 2021. Why is calcite a strong phosphorus sink in freshwater? Investigating the adsorption mechanism using batch experiments and surface complexation modeling. Chemosphere 285, 131–145.

Helsel, D.R., 2012. *Statistics for censored environmental data using Minitab and R*, 2nd ed. Wiley, Hoboken, NJ, USA. https://doi.org/10.1002/9781118162729.

Hong, Z., Zhao, Q., Chang, J., et al., 2020. Evaluation of water quality and heavy metals in wetlands along the Yellow River in henan province. Sustainability. https://doi.org/10.3390/su12041300.

House, W., Denison, F., 2002. Total phosphorus content of river sediments in relationship to calcium, iron and organic matter concentrations, 282-283 Sci. Total Environ. 81–92. https://doi.org/10.1016/S0048-9697(01)00923-8.

Islam, F.S., Gault, A.G., Boothman, C., Polya, D.A., Charnock, J.M., Chatterjee, D., Lloyd, J.R., 2004. Role of metal-reducing bacteria in arsenic release from bengal delta sediments. Nature 430 (6995), 68–71. https://doi.org/10.1038/nature02638.

Kadlec, R.H., Wallace, S.D., 2009. *Treatment wetlands*, 2nd ed. CRC Press, Boca Raton, FL, USA.

Kalani, N., Riazi, B., Karbassi, A., Moattar, F., 2021. Measurement and ecological risk assessment of heavy metals accumulated in sediment and water collected from gomishan international wetland, Iran. Water Sci. Technol. 84 (6), 1498–1508. https://doi.org/10.2166/wst.2021.317.

Karimian, N., Johnston, S.G., Burton, E.D., 2017. Effect of cyclic redox oscillations on water quality in freshwater acid sulfate soil wetlands. Sci. Total Environ. https://doi.org/10.1016/j.scitotenv.2016.12.131.

Khatri, T.B., 2013. Wetlands, biodiversity and climate change. J. Wetl. Conserv. Manag. 12 (2), 89–95. ⟨https://www.researchgate.net/publication/270127077_Wetlands_Biodiversity_and_Climate_Change⟩ (Recuperado de).

Kingsford, R.T., 2016. Wetlands: conservation's poor cousins. Aquat. Conserv. Mar. Freshw. Ecosyst. 26 (1), 1–8. https://doi.org/10.1002/aqc.2709.

Laur, N., Kinscherf, R., Pomytkin, K., Kaiser, L., Knes, O., Deigner, H.-P., 2020. ICP-MS trace element analysis in serum and whole blood. PLOS ONE 15 (5), e0233357.

Lizama-Allende, K., Ayala, J., Jaque, I., 2021. The removal of arsenic and metals from highly acidic water in horizontal subsurface flow constructed wetlands. Environ. Int. https://doi.org/10.1016/j.envint.2020.106732.

Luther, G., Church, T., 1988. Seasonal cycling of sulfur and iron in porewaters of a delaware salt marsh. Mar. Chem. 24 (2), 275–282. https://doi.org/10.1016/0304-4203(88)90100-4.

McFeeters, S.K., 1996. The use of the Normalized Difference Water Index (NDWI) in the delineation of open water features. International Journal of Remote Sensing 17 (7), 1425–1432. https://doi.org/10.1080/01431169608948714.

MINAM, 2017. Estándares de calidad ambiental para agua. Decreto supremo N° 004-2017-MINAM. Ministerio del Ambiente del Perú.

2015 MINAM. (2015). *Estrategia Nacional de Humedales del Perú*. Ministerio del Ambiente, Lima, Perú. Retrieved from https://sinia.minam.gob.pe.

Ministerio del Ambiente (MINAM). (2017). *Decreto Supremo N.° 004-2017-MINAM: Estándares de Calidad Ambiental (ECA) para Agua*. Ministerio del Ambiente, Lima, Perú. Retrieved from https://www.minam.gob.pe/disposiciones/decreto-supremo-n-004-2017-minam/.

Oyarzún, J., Oyarzún, R., 2011. Sustainable development threats, inter-sector conflicts and environmental policy requirements in the arid, mining rich, Northern Chile territory. Sustain. Dev. 19 (4), 263–274. https://doi.org/10.1002/sd.441.

Pham, V.T.B., 2020. Modification of the Canadian water quality index: case study assessment of groundwater quality in Mekong delta (Thesis). Vietnam. https://doi.org/10.25534/TUPRINTS-00014394.

Piper, A.M., 1944. A graphic procedure in the geochemical interpretation of water-analyses. Transactions, American Geophysical Union 25 (6), 914–928. https://doi.org/10.1029/TR025i006p00914.

Roman-Ross, G., Cuello, G., Turrillas, X., Fernandez-Martinez, A., Charlet, L., 2006. Arsenite sorption and co-precipitation with calcite. Chem. Geol. 233 (3–4), 328–336. https://doi.org/10.1016/j.chemgeo.2006.04.007.

Roman-Ross, G., Cuello, G.-J., Turrillas, X., Fernández-Martínez, A., & Charlet, L. (2008). *Arsenite sorption and co-precipitation with calcite*. arXiv preprint arXiv: 0801.1738.

Romero, L., Alonso, H., Campano, P., Fanfani, L., Cidu, R., Dadea, C., Rojas, R., 2003. Arsenic enrichment in waters and sediments of the rio loa basin, Chile. Environ. Geochem. Health 25 (3), 201–214. https://doi.org/10.1016/S0883-2927(03)00059-3.

Ross, A.C., et al., 2023. Seasonal water storage and release dynamics of bofedal wetlands in tropical high-Andean headwaters. Hydrological Processes 14940. https://doi.org/10.1002/hyp.14940.

Sdiri, A., Higashi, T., Hatta, T., Jamoussi, F., Bouaziz, S., 2012. Comparative study of heavy metals removal from aqueous solutions by natural limestones and dolomites. J. Hazard. Mater. 193, 62–69. https://doi.org/10.1007/s13201-012-0054-1.

Shammi, M., Rahman, M., Bodrud-Doza, M. (2019). Impacts of Salinity Intrusion in Community Health: A Review of Effectiveness of Adaptation Measures to Decrease Drinking Water Sodium (DWS) from Coastal Areas of Bangladesh. Preprints. https://dx.doi.org/10.20944/preprints201901.0066.v1.

Silva, A.P., Correia, S.B., Bernardes, M.E.C., 2021. Influence of particle morphology on heavy metal adsorption in natural sediments. Chemosphere 263, 128072 (DOI).

Stottmeister, U., Buddhawong, S., Kuschk, P., et al., 2006. Constructed Wetlands and their Performance for Treatment of Water Contaminated with Arsenic and Heavy Metals. Springer Environmental Series. https://doi.org/10.1007/978-1-4020-4728-2_27.

U.S. Environmental Protection Agency (EPA). (2022). *Edition of the Drinking Water Standards and Health Advisories Tables*. U.S. Environmental Protection Agency, Washington, DC. Retrieved from https://www.epa.gov.

Valladares, L.De. Los Santos, Kooyip, J.H.Jhoncon, Borja-Castro, L.E., Valerio-Cuadros, M.I., Valencia-Bedregal, R.A., Velazquez-Garcia, J.J., Aguilar, C.Villanueva, Barnes, C.H.W., Dominguez, A.G.Bustamante, 2022. Characterization of spanish river carbonatite (SRC) for agricultrural fertilizer. Hyperfine Interact. 243, 19. https://doi.org/10.1007/s10751-022-01803-4.

Vera-Herrera, L., Romo, S., Soria, J., 2022. How agriculture, connectivity and water management can affect water quality of a Mediterranean coastal wetland. Agronomy 12 (2), 486. https://doi.org/10.3390/agronomy12020486.

Wang, Y.-m, Wang, S.-w, Wang, C.-q, et al., 2020. Simultaneous immobilization of soil Cd(II) and As(V) by Fe-modified biochar. Int. J. Environ. Res. Public Health 17 (3), 827. https://doi.org/10.3390/ijerph17030827.

Wang, Q., Zhou, S., Song, Y., 2016. Effects of particle shape and size on the adsorption of heavy metals by natural sediments. Environ. Sci. Pollut. Res. 23 (24), 24652–24661.

Wetlands International. (2024). High Andean wetlands under pressure: Regional assessments of salinization and climate impacts. Wetlands International. Retrieved September 11, 2025, from https://www.wetlands.org.

WHO, 2017. Guidelines for Drinking-water quality. 4Th edition. Incorporating the 1st addendum. World Health Organization. ⟨https://www.who.int/water_sanitation_health/dwq/fulltext.pdf⟩.

Xi, Y., Peng, S., Ciais, P., Chen, Y., 2021. Future impacts of climate change on inland ramsar wetlands. Nat. Clim. Change 11 (6), 474–479. https://doi.org/10.1038/s41558-020-00942-2.

Xu, H., 2006. Modification of normalised difference water index (NDWI) to enhance open water features in remotely sensed imagery. Int. J. Remote Sens. 27 (14), 3025–3033. https://doi.org/10.1080/01431160600589179.

Zhang, X., Liu, Y., Zhao, W., Li, J., Xie, S., Zhang, C., He, X., Yan, D., Wang, M., 2023. Impact of hydrological changes on wetland landscape dynamics and implications for ecohydrological restoration in honghe national nature reserve, northeast China. Water 15 (19), 3350. https://doi.org/10.3390/w15193350.

Zhao, Y., Wu, S., Yu, M., Zhang, Z., Wang, X., Zhang, S., Wang, G., 2020. Seasonal iron-sulfur interactions and the stimulated phosphorus mobilization in freshwater lake sediments. Sci. Total Environ. 738, 144336. https://doi.org/10.1016/j.scitotenv.2020.144336.

Zhu, W., Bian, B., Hu, S., 2019. Characteristics of heavy metal adsorption onto sediment particles: influence of particle size, shape, and mineralogy. J. Environ. Sci. 84, 174–184.

Zhu, S., Mostafaei, A., Luo, W., Jia, B., Dai, J., 2019. Assessing water quality for urban tributaries of the three gorges reservoir, China. Water Resour. Dev. 9 (1), 105–115. https://doi.org/10.2166/WRD.2018.010.